Narrow dip in the angular dependence of the irreversible magnetic moment in columnar-defected $YBa_2Cu_3O_y$ single crystals

A. A. Zhukov
Physics Department, Moscow State University, Moscow 117234, Russia

G. K. Perkins, L. F. Cohen, and A. D. Caplin
Centre for HTS, Blackett Laboratory, Imperial College, London SW7 2BZ, United Kingdom

H. Küpfer and T. Wolf
Forschungszentrum Karlsruhe, Institut für Technische Physik, Postfach 3640, D-76021 Karlsruhe, Germany

G. Wirth
Gesellschaft für Schwerionenforschung mbH, Planckstrasse 1, D-64291 Darmstadt, Germany
(Received 9 April 1998)

When the magnetic field H is rotated around the axis parallel to the short side of columnar-defected $YBa_2Cu_3O_y$ single crystals, we observe a narrow dip in the irreversible magnetic moment for H parallel to the columns. The conditions for the existence of this phenomenon have been clarified by investigating different sample geometries and field orientations. Using the anisotropic critical state model, we show that the anomaly arises from a sharp increase of the critical current density parallel to the field rotation plane. Possible explanations for the underlying vortex dynamics are discussed. [S0163-1829(98)04237-4]

I. INTRODUCTION

The enhancement of vortex pinning in high-temperature superconductors (HTS's) by columnar defects is well established.[1] There have been some studies[2] of how the direction of magnetic field effects the vortex-column interaction, but with limited ($\sim 1°$) angular resolution. Recently,[3] using vector magnetometry with high angular resolution, the transformations of the vortex structure in columnar defected $YBa_2Cu_3O_y$ single crystals were studied. It was found that the behavior of the reversible transverse magnetization related to the direction of vortices, corresponds to the generally accepted physical picture of vortex lock-in phenomena. When the angle φ between the column direction and the magnetic field $\boldsymbol{H}$ is less than the lock-in angle φ_L, vortices are locked to the column direction. For larger angles $\varphi_L < \varphi < \varphi_T$, the vortex structure is kinked. Finally, when $\varphi > \varphi_T$, the vortices become rectilinear and closely parallel to $\boldsymbol{H}$.

Thus for small φ, vortex pinning by columns is much stronger than bulk pinning by point defects, but at large φ the columns become ineffective. The critical current density J_C should therefore decrease rapidly with increasing φ; equivalently, there should be a peak in the irreversible magnetic moment $m_{\rm irr}(\varphi)$ at $\varphi = 0$. This was indeed reported previously. However, in this work we found that over a substantial portion of the field-temperature plane, there is a *minimum* of $m_{\rm irr}(\varphi)$ instead of a maximum at $\varphi = 0$, but only for certain orientations of the field rotation plane with respect to the sample geometry. Here we explore this unexpected phenomenon in detail, present a phenomenological interpretation, and discuss its possible physical origin.

II. EXPERIMENTAL

A. Samples

We have studied five twinned $YBa_2Cu_3O_y$ single crystals taken from a single batch, which were characterized magnetically prior to irradiation. At 77 K they displayed no ''fishtail'' peak and the shielding current density was below 10^4 A/cm^2, indicative of little pinning in the virgin state. In four crystals (*AH*, *AE*, *HA*, and *AW*), columnar defects were created by 2.2 GeV Au ion irradiation; for crystal *I2*, 2.7 GeV U ions were used. As is usual, the irradiation direction was tilted slightly ($\sim 1°$), away from the c axis to avoid channeling. All samples are rectangular in shape; their dimensions and irradiation fluences, expressed as matching field $\boldsymbol{B}_\psi$, are listed in Table I.

B. Alignment procedure

The effects that we are concerned with here occur over a narrow range of angle between the applied field $\boldsymbol{H}$ and the column direction. We use a vibrating sample magnetometer equipped with two perpendicular pickup coils that simulta-

TABLE I. Dimensions and matching fields of the irradiated crystals.

Sample number	l mm	s mm	t μm	$\eta = l/s$	Matching field/T
AH	1.26	0.57	25	2.21	3
AE	1.12	0.72	27	1.47	1
HA	1.25	0.9	25	1.38	0.3
AW	1.4	0.75	20	1.87	0.1
I2	1.76	0.54	38	3.26	0.04

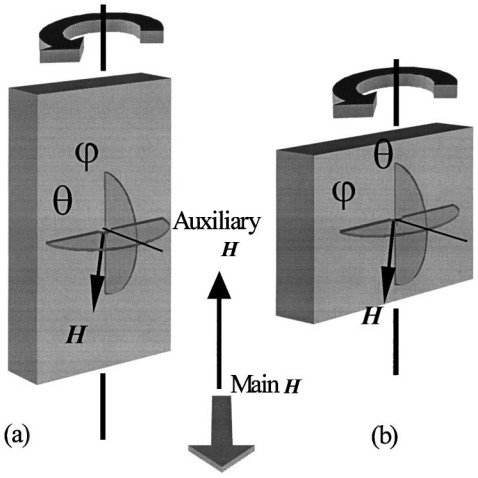

FIG. 1. Geometry of the angular studies. (a) Rotation axis parallel to the long l is denoted by θ; (b) rotation of the applied field $\boldsymbol{H}$ by the axis parallel to the short sample side s is denoted by the angle φ.

neously measure m_{std} and m_{ort} the components of the magnetic moment parallel and perpendicular to the applied (horizontal) magnetic field, respectively. The sample can be rotated about a vertical axis (Fig. 1) with high angular resolution (0.01°) and reproducibility,[4] but the uncertainties in sample mounting and in column direction may cause the latter to be tipped out of the horizontal plane by up to ~1° or so. Later we added a vertical solenoid, swept synchronously with the main horizontal superconducting coils, to tilt the field rotation plane into alignment with the columns. This tilt range is limited by dissipation in the secondary solenoid, which can generate a maximum vertical field of ~40 mT.

Within the horizontal plane, the column direction can be readily identified, either through a *null* in the *reversible* part of the moment transverse to $\boldsymbol{H}$, or an *extremum* in the *irreversible* moment parallel to $\boldsymbol{H}$.[3] As the direction of the *ab* planes can also be determined in a similar manner, we can find the misalignment (~1°) between the projections of the columns and *c* axis to the rotation plane with an accuracy better than 0.1°. As we found it of no importance for the results presented here, we will further assume that *c* axis coincides with the direction of the columns which was used as the zero angle reference direction.

As we shall see below, the observed behavior depends critically on whether the field rotation axis is parallel to the long side or to the short transverse side of the thin platelike sample (Fig. 1). For investigations over a substantial angular range, the sample does have to be remounted, and the column direction relocated for the second set of measurements. By using the secondary solenoid, data could be obtained for both rotation planes within a limited angular window without remounting the sample.

In presenting and analyzing the data, it is convenient to distinguish field rotations in the two orthogonal planes by denoting the angles as φ and θ for the rotation axis parallel to the short and long side of the sample, respectively (Fig. 1). In what follows we shall refer to these as the short and long rotation axes.

C. Measurement regime

In the present study, we are concerned with flux pinning as reflected by shielding currents, which generate an *irreversible* moment $\boldsymbol{m}$; we obtain $\boldsymbol{m}$ from the difference between the upward and downward legs of the magnetization loops. As we have pointed out previously,[5] for $\boldsymbol{H}$ applied at an arbitrary angle, the shielding currents in a thin plate superconductor are closely confined to the plane of the plate, unless $\boldsymbol{H}$ is very nearly parallel to the plate. The associated moment $\boldsymbol{m}$ is therefore nearly parallel to the plate normal; we obtain its magnitude from the vector addition of the measured moments m_{std} and m_{ort}. However, similar behaviour can also be deduced from m_{std} alone.

We need to avoid the complications arising from demagnetizing effects, so all the results reported here are at fields large compared with the critical state full penetration field $\boldsymbol{H}_{\mathrm{pen}}$. The latter is proportional to the critical current density j, which itself varies greatly between our samples because of their wide range of fluences. Consequently, the regions of the field-temperature plane that have been examined are not the same for all samples.

The data presented here arise from φ scans with θ set to 0°, and vice versa, although in setting the sample alignment and for other reasons, we have explored other orientations close to the column direction. Our procedure was always to fix an orientation, and then measure a magnetization loop; the converse protocol, with sample rotation in fixed field can readily generate artifacts.[5] While some flux creep is always present, the features reported here are not sensitive to it, as checked by performing magnetization loops at widely different sweep rates.

III. RESULTS

Figure 2 shows the angular dependences of $\boldsymbol{m}$ for samples *HA*, *AH*, and *I*2. Over a broad angular range, the moment increases as the field direction approaches that of the columns, as seen previously.[2] However, for φ scans (short rotation axis), there is a narrow dip in magnetic moment at $\varphi = 0$ evident in all samples, although somewhat broader for the sample with the lowest fluence *I*2. This minimum was found to exist only below a threshold field $\mu_0 H_b$, which decreases with increasing temperature, and which can be greater or smaller than the matching field $\boldsymbol{B}_\Psi$. For $\mu_0 \boldsymbol{H} > \mu_0 \boldsymbol{H}_b$ no dip is present.

Furthermore, at a given field, the presence of a minimum depends on the rotation plane with respect to the sample geometry [Fig. 2(b)]: Samples of large aspect ratio (*AH* and *I*2) exhibit no dip at all for θ scans (long rotation axis), while *HA*, which is almost square, shows a dip in $\boldsymbol{m}(\theta)$ similar to that seen in $\boldsymbol{m}(\varphi)$. These curves are not perfectly symmetric about the origin (the column direction); this may result from the deliberate small misalignment between the irradiation direction and the *c*-axis and the uncertainty in setting the rotation plane (Sec. II A).

Data obtained on samples *AW* and *AE* with the secondary coil, so that θ and φ could both be scanned *in situ*, are presented in Fig. 3. As in the initial (and less precisely aligned) measurements described above, the dip is observed in $m(\varphi)$ for all cases, but the dip in $m(\theta)$ occurs only for the almost-square sample *AE*. To summarize, all five samples show a

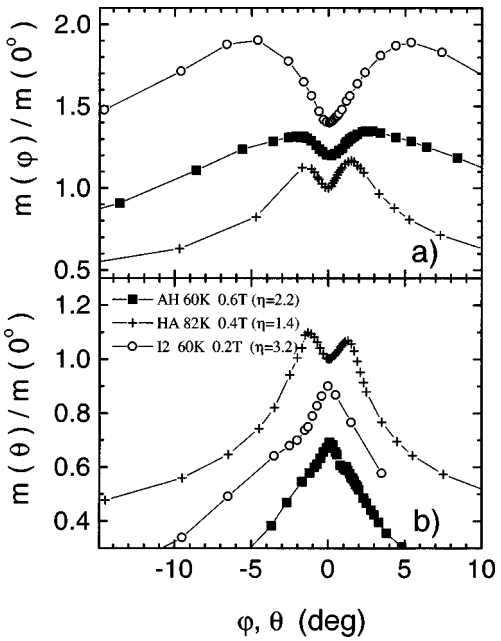

FIG. 2. The angular dependences of the normalized irreversible magnetic moments of samples *AH*, *HA*, and *I2* (a) for rotation axis parallel to the short sample side $\boldsymbol{m}(\varphi)/\boldsymbol{m}(0)$, and (b) for rotation axis parallel to the long sample side $\boldsymbol{m}(\theta)/\boldsymbol{m}(0)$. For clarity, the curves have been displaced vertically. These data were taken prior to the incorporation of the secondary solenoid (Sec. II B), so that the alignment of the column direction to the field rotation plane is not better than about 1°.

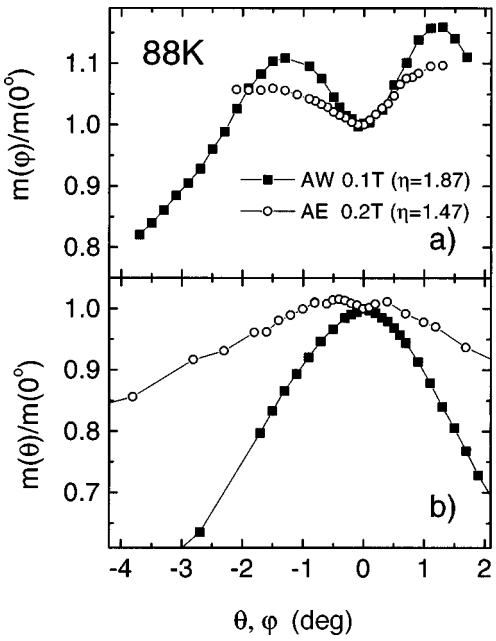

FIG. 3. The angular dependences of the normalized irreversible magnetic moments of samples *AW* and *AE*, measured with the additional vertical solenoid to obtain more accurate alignment (see text). (a) $\boldsymbol{m}(\varphi)/\boldsymbol{m}(0)$; (b) $\boldsymbol{m}(\theta)/\boldsymbol{m}(0)$.

central minimum when $\boldsymbol{H}$ is rotated around the short axis of the sample, but for rotation around long axis, the minimum occurs only in samples that are nearly square.

IV. MODEL

A. Symmetry breaking

Because these crystals are twinned, on a mesoscopic scale they should have four-fold symmetry in the *ab* plane prior to irradiation. That symmetry is broken, but only weakly, by the deliberate small misalignment between the *c*-axis and the irradiation direction (Sec. II A). We can exclude this factor as the reason for the observed behavior because of the importance of the sample geometry found in the data, and also because no significant anisotropy in the *ab* plane induced by columnar defects has ever been reported (e.g., Ref. 6 and references therein).

On a macroscopic scale, the rectangular shape of these platelike crystals is strongly symmetry breaking, and indeed that is the correlation we observe: a simple maximum in $\boldsymbol{m}$ occurs only if $\boldsymbol{H}$ is rotated by axis parallel to the long side of markedly rectangular crystals; otherwise there is a central minimum. We therefore look at the interplay between the field direction and the macroscopic shielding currents.

When $\boldsymbol{H}$ is parallel to the normal, the shielding currents in a rectangular superconducting plate that flow parallel to the long and short sides of the sample are mesoscopically equivalent. However, as $\boldsymbol{H}$ is rotated, this equivalence breaks down: the current (density) $\boldsymbol{j}_{\parallel}$ parallel to the rotation plane acquires a component in the direction of $\boldsymbol{H}$, whereas the current $\boldsymbol{j}_{\perp}$ perpendicular to the rotation plane remains orthogonal to $\boldsymbol{H}$ (Fig. 4). Below we consider the anisotropic Bean model and show that the observed symmetry breaking can be related to anisotropy in the shielding currents induced when the magnetic field is tilted.

B. The anisotropic critical state model

The standard Bean critical state model was extended some time ago to include anisotropic critical current densities in a rectangular plate with magnetic field applied parallel to the normal.[7,8] More recently, we have shown that for fields tilted from the normal, over a large angular range $\boldsymbol{m}$ is dominated totally by the in-plane currents.[5] This result was obtained in the closed form for an infinite strip. Assuming that it remains valid for a finite rectangular slab, the standard anisotropic critical state model can be used also when $\boldsymbol{H}$ is tilted away from the normal. In this case the angular dependence of the magnetic moment is caused by the angular dependence of the in-plane currents.

We distinguish rotation axes parallel to the short and long sample sides by denoting the angles from the normal as φ and θ (Fig. 1); mesoscopically these are equivalent, so that the angular dependence of the current is independent of the orientation of the sample sides, i.e., $j_{\parallel}(\varphi)\equiv j_{\parallel}(\theta)$ and $j_{\perp}(\varphi)\equiv j_{\perp}(\theta)$.

Then for small angles of tilt, the current anisotropy $k=j_{\parallel}/j_{\perp}$ will be close to unity, and so less than the sample aspect ratio $\eta(=l/s)$; the pattern of current flow will be that indicated in Fig. 4(a). The magnetic moments are

$$m(\varphi)=\frac{j_{\parallel}(\varphi)s[3\eta-k(\varphi)]}{6\eta}V, \tag{1}$$

$$m(\theta)=\frac{j_{\perp}(\theta)s[3\eta-k^{-1}(\theta)]}{6\eta}V, \tag{2}$$

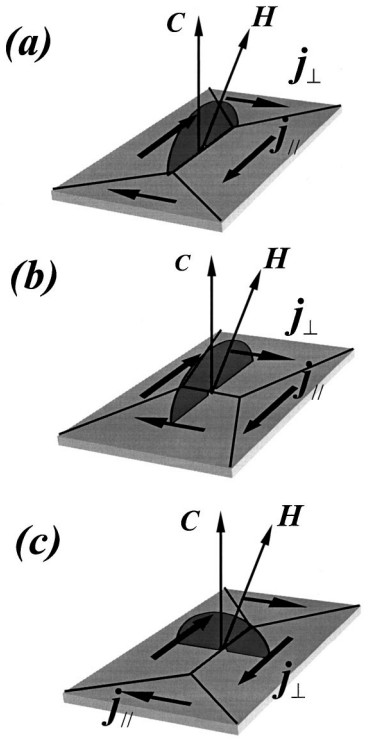

FIG. 4. The ''rooftop'' pattern of distribution of shielding currents in a rectangular sample. The critical current (density) in the plane of the sample that flows perpendicular to $\boldsymbol{H}$ is denoted $\boldsymbol{j}_\perp$, that with a component parallel to $\boldsymbol{H}$ is $j_\parallel$. Because the anisotropy of the currents $j_\parallel/\boldsymbol{j}_\perp$ increases with increasing tilt angle, the initial pattern (a) eventually switches to that of (b) when $\boldsymbol{H}$ is rotated around short axis. In contrast, for rotations around long axis (c), the initial pattern remains stable.

where V is the sample volume.

Particularly, for small changes in the currents near $(\theta,\varphi)=0$ when $\boldsymbol{j}_\parallel(\varphi)=\boldsymbol{j}_\parallel(0)(1+\beta_\parallel)$ and $\boldsymbol{j}_\perp(\varphi)=\boldsymbol{j}_\perp(0)(\mathbf{1}-\beta_\perp)$, with $\beta_\perp,\beta_\parallel \ll 1$ (this choice of signs will be seen later to be convenient), we find

$$\mu(\varphi)=m(\varphi)/m(0)\approx 1+\beta_\parallel-\frac{\beta_\parallel+\beta_\perp}{3\eta-1}, \tag{3}$$

$$\mu(\theta)=m(\theta)/m(0)\approx 1-\beta_\perp+\frac{\beta_\parallel+\beta_\perp}{3\eta-1}. \tag{4}$$

At larger tilt angles φ the anisotropy of the currents $k(\varphi)$ increases, and when $k\geqslant\eta$ the ''rooftop'' pattern of current flow alters to that of Fig. 4(b). Equation (1) must then be replaced by

$$m(\varphi)=\frac{j_\perp(\varphi)l[3-\eta k^{-1}(\varphi)]}{6}V. \tag{5}$$

Equation (2) remains valid.

C. Behavior for *H* nearly parallel to the columns

The presence of a minimum in square samples ($\eta=1$) when $\boldsymbol{H}$ is rotated from the normal requires $\beta_\parallel(\varphi)>\beta_\perp(\varphi)$ [Eqs. (3) or (4)]; furthermore, when η increases, the behaviour of $m(\varphi)$ as $\boldsymbol{H}$ is rotated around the short axis becomes

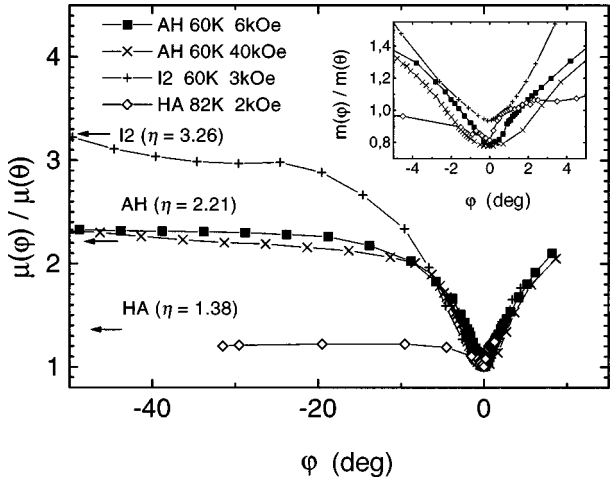

FIG. 5. The ratio of the normalized magnetic moments $\mu(\varphi)/\mu(\theta)$ for equal tilt angles ($\varphi=\theta$) in the two rotation planes. At high angles, $\mu(\varphi)/\mu(\theta)$ is seen to tend toward the sample aspect ratio η. The inset shows the behavior of $\boldsymbol{m}(\varphi)/\boldsymbol{m}(\theta)$ at small angles.

dominated by $\beta_\parallel(\varphi)$ [Eq. (3)]. Therefore, the experimental observation that there is always a central minimum in these φ scans [Figs. 1(a) and 2(a)] shows that for small φ, $j_\parallel(\varphi)$ increases more rapidly than $j_\perp(\varphi)$ decreases.

For the θ scans [Eq. (4)] initially $m(\theta)$ has a central minimum if $3\eta\leqslant 2+[\beta_\parallel(\varphi)/\beta_\perp(\varphi)]$. Although we cannot expect $\beta_\parallel(\varphi)$ and $\beta_\perp(\varphi)$ to be quantitatively the same in all our samples, because of their wide range of fluences, the fact that the samples with $\eta\leqslant 1.5$ show central minima in the θ scans, but those with $\eta\geqslant 1.5$ have central maxima [Figs. 2(b) and 3(b)], suggests that for small φ, $\beta_\parallel(\varphi)$ is typically up to 2.5 times larger than $\beta_\perp(\varphi)$.

D. Behavior for *H* at large angles to the normal

For current $j_\parallel(\varphi)$ the Lorentz force decreases with φ. This, and other reasons discussed below, determine the fast increase of the anisotropy k. Because the samples studied here have moderate values of η, for any given sample the anisotropy k of the currents will at some angle φ_c exceed its geometrical aspect ratio η. In which case Eq. (5) applies instead of Eq. (1), and the current pattern of Fig. 4(b) replaces that of Fig. 4(a). Thereafter both $m(\varphi)$ and $m(\theta)$ will be dominated by $j_\perp$, which decreases with increasing angle. The position of the subsidiary maxima in the φ scans is a measure of φ_c, so that again with the *caveat* that the samples cover a range of fluences and matching fields, it is consistent that the larger the aspect ratio, the greater the angle of these maxima [Fig. 2(a)].

One further result of the anisotropic critical state model is that when the angles φ and θ become large, so that the anisotropy k is large, the angular ratio of the magnetic moments $\nu(\varphi)=\boldsymbol{m}(\varphi)/\boldsymbol{m}(\theta=\varphi)$ [Eqs. (2) and (5)] tends towards the sample aspect ratio η [recalling that $j_\perp(\varphi)\equiv j_\perp(\theta)$]. Here we use φ to represent angular dependences in different directions without reference to the scan direction. The data shown in Fig. 5 demonstrate the quantitative validity of the model. Small misalignment ($<1°$) of the rotation plane and columns leads to the uncertainty ($\sim$10–20%, see inset in Fig. 5) in the values of $m(\varphi=0°)$ and $m(\theta=0°)$ that are ob-

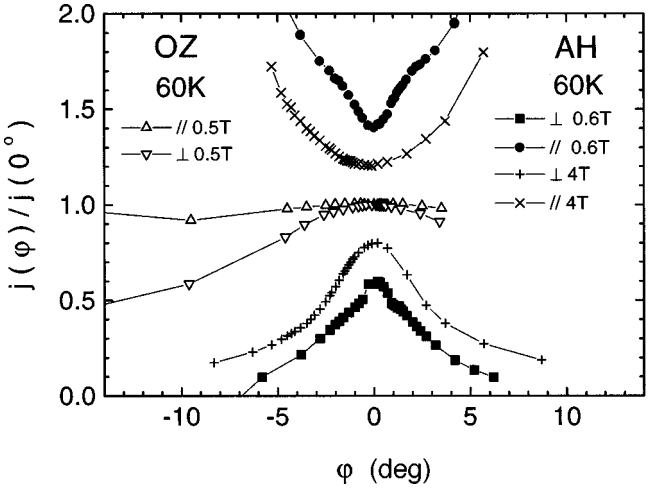

FIG. 6. The normalized angular dependences of the currents parallel $\boldsymbol{j}_{\parallel}$ and perpendicular $\boldsymbol{j}_{\perp}$ to the rotation plane of $\boldsymbol{H}$, as obtained from the measured magnetic moments via Eqs. (6) and (7). Data are shown for the irradiated crystal *AH* at two different fields, and for comparison, an unirradiated crystal (*OZ*). For clarity, the curves have been displaced vertically.

tained in two separate experiments with sample remounted. To cancel the uncertainty we used normalization by these values and considered ratio of $\mu(\varphi,\theta)=m(\varphi,\theta)/m(0°)$.

E. Angular dependences of the current densities

The critical state equations for $\boldsymbol{m}(\varphi)$ and $\boldsymbol{m}(\theta)$ [Eqs. (1), (2) or (5)] can be inverted to extract the angular variations of $j_{\perp}$ and $j_{\parallel}$. For $\nu<2\eta^3/(3\eta^2-1)$ the anisotropy k can be calculated from the cubic equation

$$k^3(\varphi)-3\eta k^2(\varphi)+3\eta\nu(\varphi)k(\varphi)-\nu(\varphi)=0, \qquad (6)$$

where only one physical solution exists for the range $1<k<\eta$. Once k is found (using the standard solution[9]) the values of the currents $j_{\parallel}$ and $j_{\perp}$ can be found straightforwardly from Eqs. (1) and (2), respectively. For large $\nu\geqslant 2\eta^3/(3\eta^2-1)$ the anisotropy $k\geqslant\eta$ can be calculated using

$$k(\varphi)=\frac{\nu(\varphi)-\eta^3}{3\eta[\nu(\varphi)-\eta]}, \qquad (7)$$

and the currents $j_{\parallel}$ and $j_{\perp}$ are determined from the Eqs. (5) and (2), respectively.

The results for a typical irradiated sample are shown in Fig. 6; the accuracy in the calculation of $j_{\parallel}$ decreases rapidly as φ increases so the data shown are restricted to small angles. For comparison, data are included also from an unirradiated twinned crystal in which the pinning is dominated by twin boundaries. This comparison stresses that the features discussed here are characteristic of irradiated samples only.

For low fields, the current density parallel to the field rotation plane, $j_{\parallel}$, increases more rapidly in the columnar-defected crystal than $\boldsymbol{j}_{\perp}$ decreases, which is the condition for a central minimum in $\boldsymbol{m}(\varphi)$ noted in Sec. IV B; the converse is the case at high fields, so there is then a central maximum in $\boldsymbol{m}(\varphi)$. In the unirradiated crystal, $j_{\parallel}$ is essentially independent of angle.

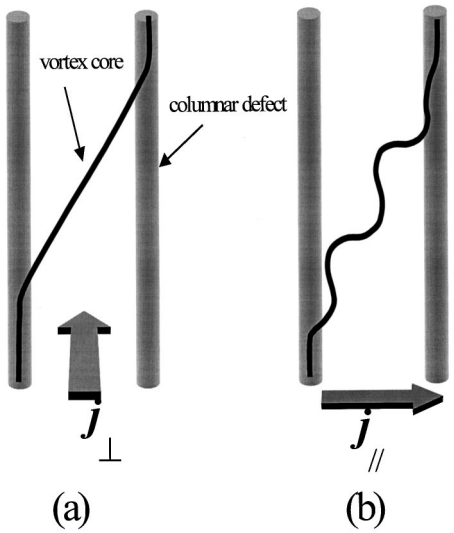

FIG. 7. Schematic vortex structure in tilted field. (a) For small tilt angles, the vortex structure consists of segments locked to the columns, linked by segments between the columns. (b) Because the links have a component parallel to the current $\boldsymbol{j}_{\parallel}$, a helical instability may arise.

V. DISCUSSION

The analysis of our data into the current components parallel and perpendicular to the rotation plane of the applied field shows that the cause for the unexpected central minimum in $\boldsymbol{m}(\varphi)$ is the rapid increase in irradiated crystals of $j_{\parallel}$ with angle, as shown in Fig. 6. For large angles, the $j_{\parallel}$ current is closely related to the Lorentz force-free configuration.[10–14] In previous experiments a large increase of the critical current for this case was observed for both conventional superconductors[10] and HTS's (Refs. 14 and 15) using transport, magnetic and magnetooptic measurements. However, it is presently unclear how this may influence the behavior at small angles.

There is of course a ''lock-in'' transition between the vortices and the columns at small enough angles, and our earlier experiments[3] indicate that for the sample shown in Fig. 6 at 60 K the boundary between the ''locked'' and ''kinked'' vortex phases occurs for a transverse field of ~20 mT, corresponding to angles φ_{L-K}, considerably smaller than the range over which $j_{\parallel}$ continues to increase. Thus, we infer that the enhancement of $j_{\parallel}$ is occurring within the ''kinked'' vortex phase.

One possibility is that because $j_{\parallel}$ contains a component which is collinear to the direction of the vortex, it could lead to helical instabilities in the vortex segments of the kinked vortex phase (Fig. 7). Such instabilities have recently been observed directly[15] and can fundamentally alter the nature of the flux pinning mechanism. The decrease of $\boldsymbol{j}_{\perp}$ as $\boldsymbol{H}$ is tilted away from the columns is related simply to the vortex-column interaction, and no helical instability is expected or observed.[15]

VI. CONCLUSIONS

When the magnetic field is rotated around the axis parallel to the short transverse side of irradiated $YBa_2Cu_3O_7$ single

crystal, we observe a narrow dip in the irreversible magnetic moment for the magnetic field direction parallel to the columns. In terms of a simple anisotropic critical state model, the minima can be understood as arising from a rapid increase in the current (density) $\boldsymbol{j}_{\parallel}$ parallel to the field rotation plane as the field is tilted, which is faster than the decrease of the perpendicular current $\boldsymbol{j}_{\perp}$. One quantitative prediction of this model is that at large angles, the ratio of these current densities should approach the sample aspect ratio η; the good agreement of the values measured gives strong support to the model.

In terms of the vortices and their interaction with the columnar defects, this behavior is occurring within the ''kinked'' vortex phase. One possibility for the contrasting behavior of $\boldsymbol{j}_{\parallel}$ and $\boldsymbol{j}_{\perp}$ is that the former is susceptible to helical instabilities, but the latter is not.

ACKNOWLEDGMENTS

The authors are grateful to E. H. Brandt, J. R. Clem, A. M. Campbell, and L. A. Ponomarenko for useful discussions. This work was supported by NATO Linkage Grant No. HT931241, the UK Engineering and Physical Sciences Research Council, the Russian Foundation for Basic Research Grant No. 96-02-18376a, the joint RFBR (Grant No. 96-02-00235G) and DFG [Grant No. 436Rus-113/417/O(R)], and INTAS Grant Nos. 97-1717 and 94-3562.

[1] L. Civale, A. D. Marwick, T. K. Worthington, M. A. Kirk, J. R. Thompson, L. Krusin-Elbaum, Y. R. Sun, J. R. Clem, and F. Holtzburg, Phys. Rev. Lett. **67**, 648 (1991); M. Konczykowski, F. Rullier-Albenque, E. R. Yacoby, A. Shaulov, Y. Yeshurun, and P. Lejay, Phys. Rev. B **44**, 7167 (1991); A. A. Zhukov, V. V. Moshchalkov, V. A. Rybachuk, V. A. Murashov, A. Yu. Martynkin, S. W. Moshkin, and I. N. Goncharov, Physica C **185-189**, 2137 (1991); W. Gerhauser, G. Ries, H.-W. Neumüller, W. Schmidt, O. Eibl, G. Saemann-Ischenko, and S. Klaumünzer, Phys. Rev. Lett. **68**, 879 (1992); V. Hardy, J. Provost, D. Groult, M. Hervieu, B. Raveau, S. Durčok, E. Pollert, J. C. Frison, J. P. Chaminade, and M. Pouchard, Physica C **191**, 85 (1992).

[2] J. R. Thompson, Y. R. Sun, H. R. Kerchner, D. K. Christen, B. C. Sales, B. C. Chakoumakos, A. D. Marwick, L. Civale, and J. O. Thomson, Appl. Phys. Lett. **60**, 2306 (1992); L. Klein, E. R. Yakoby, Y. Yeshurun, and K. Kishio, J. Appl. Phys. **75**, 6322 (1994); R. Prozorov, A. Tsameret, Y. Yeshurun, G. Koren, M. Konczykowski, and S. Bouffard, Physica C **234**, 311 (1994); R. C. Budhani, W. L. Holstein, and M. Suenaga, Phys. Rev. Lett. **72**, 566 (1994); A. Ruyter, V. Hardy, Ch. Goupil, J. Provost, D. Groult, and Ch. Simon, Physica C **235-240**, 2663 (1994); W. Jiang, N.-C. Yeh, D. S. Reed, U. Kriplani, D. A. Beam, M. Konczykowski, T. A. Tombrello, and F. Holtzberg, Phys. Rev. Lett. **72**, 550 (1994); D. Zech, S. L. Lee, H. Keller, G. Blatter, B. Janossy, P. H. Kes, T. W. Li, and A. A. Menovsky, Phys. Rev. B **52**, 6913 (1995); C. J. van der Beck, M. Konczykowski, V. M. Vinokur, T. W. Li, P. H. Kes, and G. W. Crabtree, Phys. Rev. Lett. **74**, 1214 (1995); W. S. Seow, R. A. Doyle, A. M. Campbell, G. Balakrishnan, D. McK. Paul, K. Kadowaki, and G. Wirth, Phys. Rev. B **53**, 14 611 (1996).

[3] A. A. Zhukov, G. K. Perkins, Yu. Bugoslavsky, J. Totty, L. F. Cohen, A. D. Caplin, H. Küpfer, T. Wolf, and G. Wirth, Physica C **282–287**, 2155 (1997).

[4] D. Lacey, R. Gebauer, and A. D. Caplin, Supercond. Sci. Technol. **8**, 568 (1995).

[5] A. A. Zhukov, G. K. Perkins, Yu. V. Bugoslavsky, and A. D. Caplin, Phys. Rev. B **56**, 2809 (1997).

[6] G. Szenes, Phys. Rev. B **54**, 12 458 (1996).

[7] V. V. Moshchalkov, A. A. Zhukov, V. D. Kuznetsov, V. V. Metlushko, and L. I. Leonyuk, Superconductivity: Physics, Chemistry, Technique **2**, 98 (1989).

[8] E. M. Gyorgy, R. B. van Dover, K. A. Jackson, L. F. Schneemeyer, and J. V. Waszczak, Appl. Phys. Lett. **55**, 283 (1989).

[9] G. A. Korn and T. M. Korn, *Mathematical Handbook for Scientists and Engineers* (McGraw-Hill, New York, 1961).

[10] M. A. R. LeBlanc, B. C. Belanger, and R. M. Fielding, Phys. Rev. Lett. **14**, 704 (1965); M. A. R. LeBlanc, D. LeBlanc, A. Golebiowski, and G. Fillion, *ibid.* **66**, 3309 (1991); M. A. R. LeBlanc, S. Celebi, S. X. Wang, and V. Plecácêk, *ibid.* **71**, 3367 (1993); W. E. Timms and D. G. Walmsley, J. Phys. F **5**, 287 (1975); G. Fillion, R. Gauthier, and M. A. R. LeBlanc, Phys. Rev. Lett. **43**, 86 (1979).

[11] A. M. Campbell and J. E. Evetts, Adv. Phys. **21**, 199 (1972).

[12] J. R. Clem, Phys. Rev. B **26**, 2463 (1982); J. R. Clem and A. Perez-Gonzalez, *ibid.* **30**, 5041 (1984); **33**, 1601 (1986).

[13] E. H. Brandt, Rep. Prog. Phys. **58**, 1456 (1995).

[14] M. V. Indenbom, A. Forkl, B. Ludescher, H. Kronmüller, H.-U. Habermeier, B. Leibold, G. D'Anna, T. W. Li, P. H. Kes, and A. A. Menovsky, Physica C **226**, 325 (1994); G. D'Anna, M. V. Indenbom, M.-O. André, W. Benoit, and E. Walker, Europhys. Lett. **25**, 225 (1994).

[15] M. V. Indenbom, C. J. van der Beek, V. Berseth, G. D'Anna, A. Erb, E. Walker, and R. Flükiger, Nature (London) **385**, 702 (1997).